Classical and Quantum-Mechanical Studies of Crystalline FOX-7 (1,1-Diamino-2,2-dinitroethylene)

Dan C. Sorescu,[†,‡] Jerry A. Boatz,[§] and Donald L. Thompson*[,†]

Department of Chemistry, Oklahoma State University, Stillwater, Oklahoma 74078, and Air Force Research Laboratory, AFRL/PRSP, 10 E Saturn Blvd., Edwards Air Force Base, California 93524

Received: January 24, 2001; In Final Form: March 16, 2001

First principles molecular orbital and plane-wave ab initio calculations have been used to investigate the structural and vibrational properties of the highly efficient low sensitive explosive 1,1-diamino-2,2-dinitroethylene (FOX-7) in both the gas and solid phases. The ab initio molecular orbital calculations performed at second-order (MP2) and fourth-order (MP4) Möller−Plesset levels and using density-functional theory (DFT) methods with B3LYP functional indicate that in the gas phase FOX-7 is the most stable conformer relative to its cis-1,2 and trans-1,2 isomers. The calculated MP2 and DFT structures for the FOX-7 molecule agree well with the experimental X-ray configuration but with twists of the nitro and amino groups much larger than in the solid phase. The calculated fundamental vibrational frequencies at the DFT level generally compare well with the MP2 results. The IR spectra were computed for the three isomers. The structural properties of the FOX-7 crystal have been studied by a plane-wave DFT method. These calculations were done with periodic boundary conditions in all three directions. The optimization of the crystal structure has been done with full relaxation of the atomic positions and of the lattice parameters under $P2_1/n$ symmetry. The predicted crystal structure is in good agreement with X-ray data. We have developed an intermolecular potential to describe the structure of the FOX-7 crystal in the approximation of rigid molecules. This potential is composed of pairwise exp-6 Buckingham terms and Coulombic interactions. Crystal-packing calculations without symmetry constraints performed with the proposed potential accurately reproduce the main crystallographic features and yield very good agreement with the estimated lattice energy. This intermolecular potential was further tested in isothermal−isobaric molecular dynamics simulations at atmospheric pressure and in the temperature range of 4.2−450 K. It is found that the increase of temperature does not significantly change the orientations of the molecules inside the unit cell. The thermal expansion coefficients calculated for the model indicate anisotropic behavior with the largest expansion along the *b* crystallographic direction.

I. Introduction

Several studies performed in the past decade have indicated increasing interest in the synthesis and characterization of highly energetic materials with low sensitivities.[1−4] Among them, the new explosive 1,1-diamino-2,2-dinitroethylene (FOX-7; see Figure 1) was reported recently[4] and was characterized as a promising high energy density material with superior shock-sensitivity properties. This compound is strongly dipolar and decomposes only above 220 °C.[4] The purpose of the present study was to develop a theoretical model that can be used to explore the fundamental behavior of this system and that can be used to develop a better understanding of the basic characteristics of energetic materials that determine shock sensitivity.

The structure of crystalline FOX-7 was resolved by X-ray crystallography in two independent studies.[5,6] The crystal has monoclinic $P2_1/n$ symmetry, with $Z = 4$ molecules per unit cell (see Figure 1a). The molecular geometry is characterized by extensive π conjugation, with two intramolecular hydrogen bonds between the nitro-O and the amino-H atoms. The molecular arrangement inside the crystal is that of two-dimensional wave-shaped layers (see Figure 1b), with extensive intermolecular hydrogen bonding within the layers and with simple van der Waals interactions between the layers. It has been suggested[5] that this molecular packing is essential for its low sensitivity to impact and the absence of a melting point. The type of molecular packing in crystalline FOX-7 is similar to that observed in other relatively insensitive energetic materials such as 1,3,5-triamino-2,4,5-trinitrobenzene (TATB)[7] and 5-nitro-2,4,-dihydro-3H-1,2,4-triazol-3-one (β-NTO).[8] The empirical evidence suggests that hydrogen bonding, which often leads to highly ordered layering of molecular sheets in solids, can be an important factor in determining the sensitivity of materials to shocking.

In contradistinction to the solid phase, the gas-phase properties of FOX-7 have not been investigated experimentally. A first theoretical attempt to characterize the properties of the FOX-7 molecule has been done by Politzer et al.[9] They used density-functional theory (DFT) calculations (B3P86/6-31+G**) to determine several important properties including the $C-NO_2$ and $C-NH_2$ bond dissociation energies and the heats of formation, vaporization, and sublimation.[5] More recently, the minimum energy path for unimolecular decomposition of FOX-7 has been investigated using B3LYP/6-31+G** calculations.[10] It was found that the lowest energy unimolecular decomposition

* To whom correspondence should be addressed.
† Oklahoma State University.
‡ Current mailing address: Department of Chemistry, University of Pittsburgh, Pittsburgh, PA 15260.
§ Air Force Research Laboratory, AFRL/PRSP.

10.1021/jp010289m CCC: $20.00
Published on Web 04/24/2001

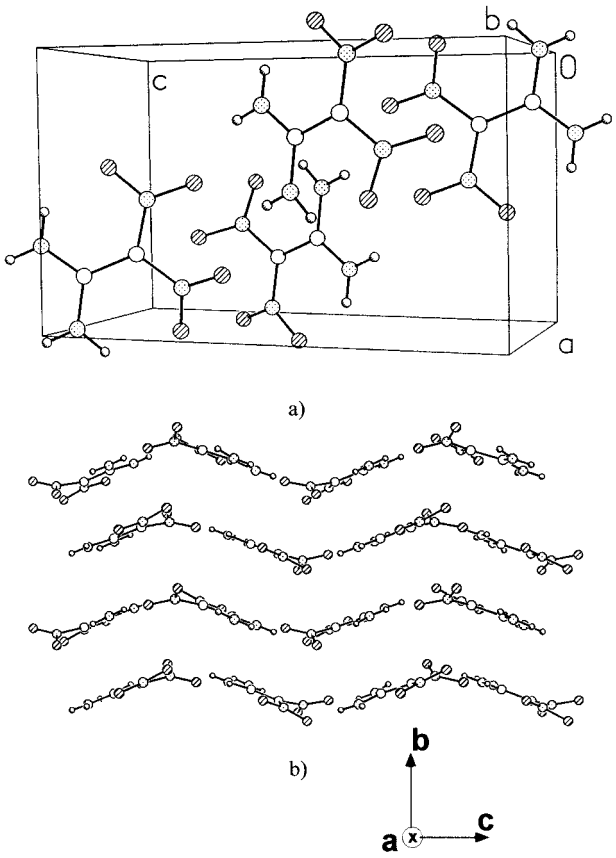

Figure 1. (a) Perspective view of the FOX-7 crystal. The H and C atoms are represented by small and large open circles, respectively, and the N and O atoms are represented by circles with a filled pattern of dots and hatching, respectively. (b) The wave-shaped layered packing viewed along (100) direction.

pathway corresponds to nitro-to-nitrite rearrangement with a calculated energy barrier of 59.1 kcal/mol. This value is very close to the experimental activation energy of 58 kcal/mol.[11]

In the present study, we extend the previous theoretical investigations by considering the effects of the crystalline field on the geometric parameters of FOX-7. For this purpose, we used first-principles calculations based on DFT and the pseudopotential method to determine the structure and electronic properties of the FOX-7 crystal. Periodic boundary conditions in all three directions were used for the present calculations. The equilibrium structure of the crystal was obtained by full relaxation of the unit cell parameters allowed by the $P2_1/n$ crystal symmetry as well as of the atomic positions inside the unit cell.

To compare the changes induced by the crystalline field upon the gas-phase structures, we have also performed ab initio calculations on the isolated FOX-7 molecule (see Figure 2a). Additionally, we have considered the stability and structural properties of two related isomers, namely, trans-1,2 and cis-1,2 (see Figure 2 parts b and c). These studies have been done on the basis of first-principles molecular orbital calculations at the MP2 and MP4[12] levels using different types of basis sets. For the purpose of comparison and as an alternative to the computationally demanding MP2 method, we have also used DFT in the Kohn−Sham formulation.[13] We have previously shown for two other highly energetic, relatively insensitive crystals, namely, NTO[14] and ANTA (3-amino-5-nitro-1,2,4-triazole),[15] that the Becke's three parameter hybrid method,[16] in combination with the Lee, Yang, and Parr correlation functional Becke3-LYP,[17] provides a similar description to that computed at the MP2 level and with the experimental values.

Besides the energetic and geometrical parameters, another set of useful data obtained from ab initio calculations are the fundamental vibrational frequencies. These were calculated for the three FOX-7 isomers using analytical second-order derivatives at the optimized geometries. The theoretical frequencies should be compared to gas-phase experimental results; however, we are not aware of any experimental measurements of the vibrational frequencies. We hope that the computed vibrational frequencies will stimulate experimental investigations of the gas-phase vibrational spectroscopy of this interesting molecule.

Ideally the equilibrium and dynamical properties of molecular crystals would be obtained from first-principles molecular dynamics simulations. Although such calculations represent the state of the art, they are computationally extremely demanding. The alternative to this approach is to develop reliable intermolecular potentials to be used in classical molecular dynamics (MD) or Monte Carlo (MC) simulations. We have successfully developed such intermolecular potentials for a series of 30 nitramine crystals,[18a−c] including some of the most important explosives such as hexahydro-1,3,5-trinitro-1,3,5-s-triazine (RDX), 1,3,5,7-tetranitro-1,3,5,7-tetraazacyclo-octane (HMX), and 2,4,6,8,-10-hexanitrohexaazaisowurtzitane (HNIW), and have analyzed the transferability of such potentials to a set of 30 nitramine crystals[18d] and 50 other nonnitramine compounds.[18e] In the present work, we report the development of an intermolecular potential to describe the structure of the FOX-7 crystal. This potential will allow direct theoretical investigations of the response of FOX-7 crystals to different external stimuli such as heating or pressure, particularly for conditions that are close to normal pressures and temperatures. In addition, the present potential model can be also used in the theoretical crystal engineering field to design new crystals with different types of molecular packing.

The methodology followed to develop this intermolecular potential is similar to that we used previously for different energetic crystals.[18] The intermolecular interactions are assumed to be describable by simple isotropic potentials such as the (6-exp) Buckingham potentials with explicit consideration of the electrostatic interactions between the charges associated with various atoms of different molecules. The Coulombic terms were determined by fitting partial charges centered on each atom of the FOX-7 molecule to a quantum mechanically derived electrostatic potential. The parametrization of the potential function was done such that the model reproduces in molecular packing (MP) calculations without symmetry constraints the experimental structure of the crystal and its lattice energy. In all of these calculations, the molecules are assumed to be rigid and the structure is described by the center-of-mass positions and the orientation parameters (the Euler angles or the set of quaternions) for each of the molecules in the unit cell. The intermolecular potential determined in MP calculations was further tested in isothermal−isobaric molecular dynamics simulations (NPT-MD) as a function of temperature over the range of 4.2−450 K at atmospheric pressure.

The organization of the paper is as follows: In section II, we present the computational methods used in the present study. In section III, we present the results of ab initio molecular orbital and total energy calculations, lattice energy minimization by molecular packing calculations without symmetry constraints, and the results of trajectories calculations in the constant temperature and pressure ensemble. Finally, we summarize the main conclusions in section V.

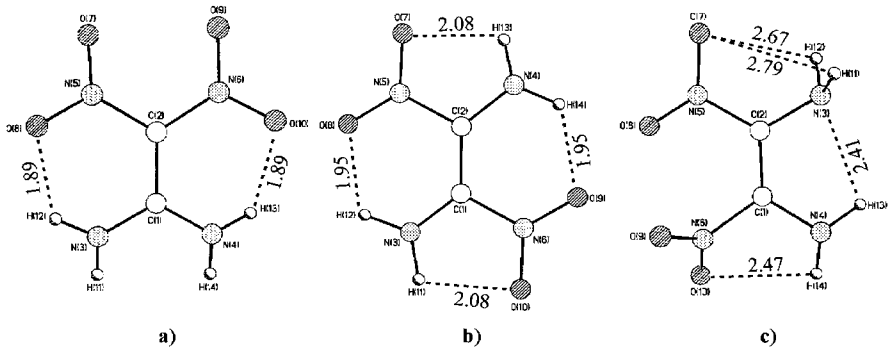

Figure 2. Schematic view of (a) the FOX-7 molecule and its (b) 1,2-*trans* and (c) 1,2-*cis* isomers. The indices for various kinds of atoms are those used consistently throughout this paper.

II. Computational Procedure

A. Ab Initio Molecular Orbital Calculations. Standard ab initio molecular orbital calculations were carried out using the Gaussian 98 suite of programs.[19] The geometries of FOX-7 and its cis-1,2 and trans-1,2 isomers have been optimized using the 6-31G** (split-valence plus d-type and p-type polarization functions) and 6-311+G** (triple-ζ-valence functions plus dp polarization and diffuse functions) basis sets.[20] The point symmetries found for the FOX-7, cis-1,2, and trans-1,2 molecules are C_2, C_1, and C_I, respectively. In the last case, the molecular symmetry was found to change from C_1 at HF level to C_I at the MP2 and B3LYP levels. All geometry optimizations met the default convergence criteria given by Gaussian 98.[19] Additionally, DFT calculations were done using B3LYP exchange-correlation functional. In this case, the geometry optimizations were performed with 6-31G** and 6-311+G** bases.

The nature of all stationary points determined at the MP2 and DFT levels has been determined by calculations of the vibrational frequencies. For all optimized geometries reported in this work, all vibrational frequencies were found to be real numbers, thus, verifying the structures as local minima. The calculated frequencies and the corresponding intensities were used to predict the IR spectra. The values of harmonic vibrational frequencies determined at different levels have been uniformly scaled by factors 0.8929 at HF/6-31G**, 0.9370 at MP2/6-31G**, and 0.9613 at both B3LYP/6-31G** and B3LYP/6-311++G**[21] to take into account the over-estimation of vibrational frequencies at these levels of theory. The vibrational modes have been characterized both quantitatively in terms of the potential energy distribution[22] over symmetry coordinates (which describes the percent contribution of the symmetry coordinates to each of the 3N-6 vibrational mode displacement vectors) and qualitatively by visual inspection of the eigenvectors of the mass-weighted MP2/6-31G** Hessian matrix.

B. Total Energy Calculations. The investigations of FOX-7 crystals have been carried out using first-principles calculations based on DFT and the pseudopotential approximation. This approach can provide an accurate description for both the isolated molecules[23] as well as the geometric and energetic properties of the corresponding molecular crystals.[24,25] In these calculations, we have used the generalized gradient approximation (GGA) with Perdew−Wang 86 exchange correlation functional.[26,27] In the pseudopotential approximation, only the valence electrons are represented explicitly, the valence-core interaction being described by ultra-soft (Vanderbilt-type) pseudopotentials[28] as provided by Kresse and Hafner.[29] These pseudopotentials permit the use of lower plane-wave cutoff energies than would be required with standard norm-conserving pseudopotentials. A pseudopotential is also used to replace the small Coulomb potential on the H atoms. The valence orbitals were expanded in a basis of plane waves with kinetic energy $\hbar^2k^2/2m < E_{cut}$, where k is the wave vector, m is the electronic mass, and E_{cut} is the chosen cutoff energy. This cutoff energy is chosen to ensure the convergence with respect to the basis set. This theoretical approach has significant advantages because of the lack of bias introduced by the choice of basis functions as well as the easy convergence to basis set completeness. The Brillouin zone was sampled with a $2 \times 2 \times 1$ mesh in the Monkhorst−Pack scheme,[30] leading to a single k point having the coordinates (0.25, 0.25, 0).

The periodic nature of the crystals has been considered by using periodic boundary conditions in all three directions. In the optimization process, all independent degrees of freedom allowed by the monoclinic $P2_1/n$ space group symmetry have been optimized. Particularly, the lattice dimensions a, b, and c; the lattice angle β; as well as all of the atomic positions inside the unit cell have been allowed to vary during the optimization process. All calculations were carried out using the Vienna ab initio simulation package (VASP).[31−33] This code searches iteratively for solution of Kohn−Sham equations[13b] via an unconstrained band-by-band minimization of the norm of the residual vector of each eigenstate and an optimized charge density mixing.

C. Molecular Packing Calculations. A general procedure for the development and testing of semiempirical intermolecular potential energy functions for organic crystals is based on molecular packing calculations.[34] The basic idea consists of minimization of the lattice energy with respect to the structural degrees of freedom of the crystal. For a crystal with Z rigid molecules per unit cell, these degrees of freedom are determined by the positions and orientations of the molecules in the unit cell as well as the dimensions and angles of the unit cell. In the present study, we have done these calculations using the algorithm proposed by Gibson and Scheraga[35] for efficient minimization of the energy of a fully variable lattice composed of rigid molecules and implemented in the program LMIN.[36]

The potential function used to describe the intermolecular interactions in the FOX-7 crystal was constructed as a sum of pairwise additive Buckingham (6-exp) (repulsion and dispersion) terms plus Coulombic (C) potentials of the forms

$$V_{\alpha\beta}^{6-\exp}(r) = A_{\alpha\beta}\exp(-B_{\alpha\beta}r) - C_{\alpha\beta}/r^6 \qquad (1)$$

and

$$V_{\alpha\beta}^{C}(r) = \frac{q_\alpha q_\beta}{4\pi\epsilon_0 r} \qquad (2)$$

where r is the interatomic distance between atoms α and β, q_α and q_β are the electrostatic charges on the atoms, and ϵ_0 is the dielectric permittivity constant of the vacuum.

The set of partial charges used in these calculations were determined through fitting these to the quantum-mechanically derived electrostatic interaction potential for an isolated molecule whose atoms are arranged in the experimental crystallographic arrangement. These calculations have been done using the CHELPG procedure as implemented in the Gaussian 98 package.[19] We have previously shown[18] for various molecular crystals that the best agreement between predicted and experimental values of crystallographic parameters and lattice energies is obtained when the set of partial charges is determined using methods that employ electron correlation effects such as MP2 perturbation theory.[12] Consequently, in the present study, the set of atom-centered monopole charges have been determined from MP2/6-31G** calculations.

The parameters $A_{\alpha\beta}$, $B_{\alpha\beta}$ and $C_{\alpha\beta}$ in the Buckingham potential, eq 1, for H and C atomic pairs are those used in our previous studies of nitramine crystals,[18a−d] whereas those for the N and O atoms have been adjusted such that the differences between the predicted and experimental geometries of the FOX-7 crystal are minimized.

Additionally we have ascertained that our potential reproduces the experimentally observed crystal symmetry by computing the symmetry operations that transform the molecules in the unit cell at the beginning and end of lattice-energy minimization. The space group was considered to be conserved if the symmetry operations, as defined in the International Tables of Crystallography,[37] between a given molecule and the remaining molecules in the unit cell remain unchanged and if the lattice parameters fixed by the lattice symmetry have not been modified significantly. If the space symmetry is not conserved as a result of energy minimization, a new space group is deduced on the basis of the final symmetry relations. It has been shown[35] that when the space group symmetry remains unchanged some of the symmetry transformations may be lost during energy minimization but are regained before convergence is attained. In the particular case of FOX-7 crystals, with space group $P2_1/n$, we found that the space group is conserved after lattice energy minimizations and that the angles α and γ of the unit cell remain very close to 90° as required by the monoclinic space group symmetry.

In addition to the condition to reproduce the lattice geometrical parameters, we imposed the condition that the calculated energy match the static lattice energy U^0 of the crystal. The lattice energy U^0 for FOX-7 can be estimated[38] on the basis of the heat of sublimation using the relation $-\Delta H_{subl} \approx U^0 + 2RT$; we used $\Delta H_{subl} = -108.8$ kJ/mol, determined by Politzer et al.,[9] using a density functional procedure.

Using the potential terms in eqs 1 and 2, the lattice energy has been evaluated as the sum of interactions between the atoms in the central unit and all of the other atoms in the image cells. For practical computational purposes, the lattice sums are evaluated over cells within a sphere centered at the origin and of radius limited by a chosen cutoff distance. The nonbonded interactions were cut off at a distance Qr^0 using a cubic feather (spline), applied over the distance $Pr^0 - Qr^0$, to ensure the continuity of the function and its first derivative. The parameters P and Q, which specify the start and the end of the cubic feather (see ref 35 for details), were set to 20.0 and 20.5, respectively. The evaluation of the Coulombic sums over the infinite periodic lattice has been done using the standard Ewald's transformation technique[35] to improve the rate of convergence of these sums. Further details of the summation procedures of different energy terms over the lattice as well as of the adjustable parameter that determines the relative contribution of the direct and reciprocal-space terms in Ewald sums are given in ref 35.

D. Constant Pressure and Temperature Molecular Dynamics Calculations. A more comprehensive test of the proposed intermolecular potential for FOX-7 crystals was done in a constant pressure and temperature (NPT) molecular dynamics simulation, in which there are no geometric constraints other than the assumption of rigid molecules. This method yields average equilibrium properties of the lattice as functions of temperature and pressure.

We have used the Nosé−Hoover barostat algorithm,[39] as implemented in the program DL_POLY_2.0,[40] to simulate the FOX-7 crystal at various temperatures in the range of 4.2−450 K and at atmospheric pressure. The equations of motion for both the translation of the rigid molecules and the simulation cell are integrated using the Verlet leapfrog scheme.[41] The molecular rotational motion is handled using Fincham's implicit quaternion algorithm.[42]

The MD simulation cell consists of a box containing 48 crystallographic unit cells (a $4 \times 4 \times 3$ box of unit cells). In the initial simulation corresponding to the lowest temperature, the position and orientation of the molecules in the unit cell were taken to be identical to those for the experimental structure. In all production runs of the Nosé−Hoover NPT ensembles, the system was integrated for 1.2×10^4 time steps (1 time step $= 2 \times 10^{-15}$ s), of which 2×10^3 steps were equilibration. In the equilibration period, the velocities were scaled after every 5 steps, so that the internal temperature of the crystal mimicked the imposed external temperature. Then, average properties were calculated over the next 10^4 integration steps in the simulation. In subsequent runs, performed at successively higher temperatures, the initial configurations of the molecular positions and velocities were taken from the previous simulation at the end of the production run.

The lattice sums were calculated subject to the use of minimum-image periodic boundary conditions in all three dimensions.[41] The interactions were determined between the sites (atoms) in the simulation box and the nearest-image sites within the cutoff distance ($R_{cut} = 10.5$ Å). In these calculations, the Coulombic long-range interaction were handled using Ewald's method.[41]

The main quantities obtained from these simulations were the average lattice dimensions and the corresponding volume of the unit cell. Additional information about the structure of the crystal has been obtained by calculating the center of mass (COM) and the site−site radial distribution functions (RDFs). These quantities have been determined from recordings done at every 10th step during the trajectory integration.

III. Results and Discussion

A. Ab Initio Molecular Orbital Calculations. *A1. Isomer Geometries.* Schematic views of the FOX-7 molecule and its trans-1,2 and cis-1,2 isomers are shown in Figure 2. The corresponding geometrical parameters of these isomers obtained by optimizations at the MP2 and B3LYP levels are given in Supplementary Tables 1S−3S. The atom designation and numbering used in these tables and in the present discussion are those indicated in Figure 2. The values given in parentheses in Tables 1S−3S represent the absolute percentage deviation of the geometrical parameters relative to the MP2/6-311+G** results, considered as reference.

As indicated by the N−C−C−N torsional angles given in Tables 1S−3S, all three bonds around the carbon atoms are almost coplanar with variations up to about ±16° from the ideal single plane. There are also small twists of NO_2 groups relative to the C−C−N (nitro) plane with deviations as high as ±16°, ±6°, and ±12° for respectively FOX-7 and its trans-1,2 and cis-1,2 isomers. However, some major differences appear in the degree of rotation out of plane of the amino group for the cis-1,2 isomer. In this case, illustrated in Figure 1c, the amino group is rotated by up to 103° relative to the C−C−N(amino) plane. This rotation away from the neighboring amino group allows formation of new hydrogen bonds that enhances the stability of this compound.

By investigating the dependence of the geometrical parameters on the basis set, we observe that at the MP2 level the bond lengths, the bond angles, and a majority of dihedral angles are practically independent of the basis set, with variations less than 1.0%. However, there is a larger effect on the twist of the nitro and amino groups relative to the N−C−C−N plane in the case of optimization with the diffuse basis set MP2/6-311+G**.

The geometrical parameters computed using B3LYP are generally very close to those obtained at the MP2 level. The maximum deviations for the bond lengths are below 1.0% at the B3LYP/6-311+G** level (except for the C−C bond in FOX-7, for which the deviation is 2.0%). For the bond angles, the corresponding maximum differences are between 2 and 4%. The largest deviations are for the torsional angles of the nitro and amino groups, with differences of up to 14−18° for the three isomers. As a result of these variations, the calculated intramolecular hydrogen bonds vary as much as 13.6% at the B3LYP/6-31G** level and 9.8% at B3LYP/6-311+G** level relative to the MP2/6-311+G** results in the case of the cis-1,2 isomer. However, for the FOX-7 and trans-1,2 molecules, the deviations of the intramolecular hydrogen bond lengths from the MP2/6-311+G** results are much smaller, with values below 6.5% and 1.4%, respectively.

A2. Isomer Energies. The absolute and relative (ΔE) energies, together with zero-point vibrational energies at various levels are given in Table 1 for the three isomers. The relative energies reported here are calculated with respect to the energy of FOX-7 as the reference. From these results, it follows that at all levels of calculation the most stable isomer is FOX-7 followed by the trans-1,2 and then cis-1,2 isomers. The trans-1,2 isomer is less stable by values ranging between 3.7 and 4.2 kcal/mol at the MP2 and MP4 levels, respectively. The DFT results are also very close to the MP4 values, ranging from 5.3 kcal/mol at the B3LYP/6-31G** and 4.6 kcal/mol at the B3LYP/6-311+G** levels. These predictions are similar to the values reported previously by Politzer et al.[9] on the basis of B3P86/6-31+G** calculations. There is a much larger spread in the energies for the cis-1,2 isomer, with values ranging from 8.3 kcal/mol at the MP4/6-311+G** level to 16.9 kcal/mol at the B3LYP/6-31G** level.

The energetic relationships seen between the three FOX-7 isomers have been previously interpreted[9] as a result of push−pull electron delocalization in competition with hydrogen-bonding stabilization. It has been shown that electronic delocalization is greatest in FOX-7 followed by the trans-1,2 isomer, whereas in the cis-1,2 isomer, it is less important because of rotations of amino and nitro groups. Our MP2/6-311+G** optimization results indicate that FOX-7 has two pairs of strong hydrogen bonds with short O···H interatomic distances of about 1.89 Å (see Figure 2). There are four such hydrogen bonds in the trans-1,2 isomer, but the O···H distances are longer than for FOX-7, with values of 1.95 and 2.08 Å, respectively, indicating weaker hydrogen bonds in the trans isomer. The cis-1,2 isomer has four hydrogen bonds but they are very weak, with O···H or N···H nonbonded distances ranging from 2.41 to 2.79 Å. Politzer et al.[9] have shown that only on the basis of the stabilization energy determined by hydrogen bonding the predicted relative stability should be cis-1,2 > FOX-7 > trans-1,2. However, the results given in Table 1 indicate that hydrogen bonding effects are less important than those due to electron delocalization. Our results predict the order of stability as FOX-7 > trans-1,2 > cis-1,2.

TABLE 1: Calculated Energies (hartrees), Energy Difference ΔE Relative to FOX-7 (kcal/mol), Unscaled Zero-Point Vibrational Energies ZPE (kcal/mol), and Total Dipole Moment (D) for FOX-7 and Its trans-1,2 and cis-1,2 Isomers

compound	calculation level[a]	energy	ΔE	ZPE	dipole
FOX-7	HF/6-31G**	−595.056 554 3		52.12	8.90
	B3LYP/6-31G**	−598.325 241 6		58.01	8.21
	B3LYP/6-311+G**	−598.507 509 7			8.55
	MP2/6-31G**	−596.736 673 5		59.46	8.52
	MP2/6-311+G**	−597.027 847 9			8.33
	MP4/6-311+G**	−597.135 815 5			8.33
trans-1,2 FOX-7	HF/6-31G**	−595.035 967 5	12.9	63.41	1.47
	B3LYP/6-31G**	−598.316 815 5	5.3	57.47	0.00
	B3LYP/6-311+G**	−598.500 160 9	4.6		0.00
	MP2/6-31G**	−596.730 414 1	3.9	58.89	0.00
	MP2/6-311+G**	−597.021 883 0	3.7		0.00
	MP4/6-311+G**	−597.128 982 4	4.2		0.00
cis-1,2 FOX-7	HF/6-31G**	−595.030 055 1	16.6	63.53	6.54
	B3LYP/6-31G**	−598.298 185 3	16.9	57.83	6.13
	B3LYP/6-311+G**	−598.482 865 0	15.4		6.67
	MP2/6-31G**	−596.719 157 0	11.0	59.00	6.54
	MP2/6-311+G**	−597.013 251 6	9.2		6.81
	MP4/6-311+G**	−597.122 494 8	8.3		6.81

[a] All computed values are for optimizations at the indicated level except for the MP4/6-311+G** calculations which have been done at the optimized MP2/6-311+G** structures.

The dipole moments for the three isomers calculated at the HF, MP2, MP4, and B3LYP levels are given in Table 1. FOX-7 is a strongly dipolar compound with a predicted dipole moment between 8.2 and 8.5 D, which is in accord with the conclusion based on experiments that the molecule possesses a large dipole.[4] The trans isomer has C_I symmetry and thus does not have a dipole moment. An exception to this is obtained at the HF/6-31G** level, where the trans isomer is found to have C_1 symmetry. Also, we find large dipole moments, values between 6.1 and 6.8 D, for the cis isomer.

A3. Isomer Frequencies. The ab initio calculated fundamental vibrational frequencies of the FOX-7 isomers are given in Table 2. The frequencies in Table 2 have been scaled by the empirical factors given in section II to correct for the over-estimation at these levels of theory. To the best of our knowledge, there are no experimental values of the fundamental frequencies available for either the gas or solid phases of FOX-7. We will consider the frequencies determined at the MP2/6-31G** level as reference. We present in Figure 3 the simulated IR spectra calculated at the MP2/6-31G** level for all three isomers.

In the case of the FOX-7 isomer, approximate assignments of the fundamental modes are given in the second column of Table 2. These assignments are based on visual inspection of the MP2/6-31G** eigenvectors and calculation of the potential energy distribution (PED) over symmetry coordinates. The PED in Table 2 shows that most of the vibrational modes in FOX-7 are quite delocalized, each involving several symmetry coor-

TABLE 2: Harmonic Vibrational Frequencies (cm^{-1}) Calculated at the MP2/6-31G Level for FOX-7 (I) and Its cis-1,2 (II) and trans-1,2 (III) isomers**

mode	assignment[a]	I	II	III
ν_1	NO_2 torsion **47.1(36) + 44.8(35) + 5.8(34)**	58.1 (B)	36.0	53.7 (A_u)
ν_2	skeletal def **34.8(17) + 29.7(18) + 22.5(14) + 11.2(15)**	108.1 (A)	75.2	100.8 (A_g)
ν_3	NH_2 wag **59.4(14) + 16.9(16) + 12.2(18) + 7.1(17)**	130.8 (A)	96.1	112.0 (A_u)
ν_4	skeletal def. **29.6(31) + 25.6(32) + 20.8(35) + 20.3(36)**	154.5 (B)	199.4	259.2 (A_u)
ν_5	C−NO_2 def **42.6(15) + 20.0(9) + 17.0(17) + 8.1(12)**	276.0 (A)	221.6	301.5 (A_g)
ν_6	C−NO−C−NH def. **35.6(33) + 26.9(26) + 11.8(34) + 5.8(32)**	310.5 (B)	224.2	323.7 (A_u)
ν_7	C−NH2 def **46.3(25) + 21.2(30) + 12.5(29) + 10.6(34)**	387.0 (B)	297.0	398.2 (A_g)
ν_8	NH-as-wag **87.4(15) + 7.3(10)**	395.4 (A)	336.5	419.3 (A_u)
ν_9	NH-s-wag **88.8(33)**	437.4 (B)	358.8	433.2 (A_g)
ν_{10}	skeletal breathe **38.1(15) + 34.5(13) + 12.3(12) + 5.0(5)**	459.3 (A)	380.8	452.3 (A_u)
ν_{11}	skeletal def **19.8(35) + 19.0(29) + 17.0(31) + 14.7(32) + 7.7(33) + 7.1(36) + 5.7(33)**	480.9 (B)	460.5	468.0 (A_g)
ν_{12}	H−N−C−C torsional **92.0(15)**	490.7 (A)	478.9	475.4 (A_g)
ν_{13}	NH_2 def. **88.3(16) + 5.6(10)**	592.9 (A)	578.4	533.8 (A_u)
ν_{14}	NH_2 rock **79.0(16) + 8.3(11)**	618.3 (A)	646.1	593.5 (A_u)
ν_{15}	$N_5-C_2-N_6$ op def. **38.6(32) + 29.4(34) + 10.0(36) + 7.8(35) + 7.8(33) + 5.5(31)**	624.7 (B)	691.1	601.0 (A_g)
ν_{16}	N_3-H_{12},N_4-H_{14} wag **87.0(34) + 5.0(33)**	689.6 (B)	715.8	696.5 (A_g)
ν_{17}	C−NO_2 def. **53.5(36) + 22.8(31) + 16.4(32)**	726.0 (B)	745.1	701.3 (A_g)
ν_{18}	C−NO_2 def +N−C−C−N def **61.1(18) + 22.8(17) + 9.7(14)**	738.2 (A)	770.2	709.3 (A_u)
ν_{19}	C−NO_2 bend **36.5(30) + 20.7(26) + 11.0(25) + 7.0(36) + 6.9(29) + 6.3(34)**	794.2 (B)	850.4	731.1 (A_u)
ν_{20}	C−NO_2-bend **42.2(12) + 20.6(13) + 13.2(5)**	861.9 (A)	881.3	850.6 (A_g)
ν_{21}	N−H bend **54.6(11) + 24.0(10) + 14.3(2)**	1104.4 (A)	981.1	953.0 (A_u)
ν_{22}	NH_2 bend **43.4(27) + 42.6(28)**	1126.6 (B)	1171.9	1069.5 (A_g)
ν_{23}	skeletal def+NH_2 rock **29.6(27) + 22.9(28) + 16.0(26) + 10.0(22) + 8.1(25)**	1178.1 (B)	1265.5	1246.6 (A_u)
ν_{24}	N−C str + NH bend **40.2(10) + 33.8(11)**	1250.7 (A)	1295.1	1310.4 (A_g)
ν_{25}	skeletal def. **33.3(22) + 16.7(29) + 14.7(24) + 9.3(23) + 7.3(27) + 6.3(28)**	1378.2 (B)	1366.3	1339.5 (A_u)
ν_{26}	C−NO_2 sym. str **32.4(5) + 21.0(7) + 19.9(13) + 11.8(6) + 5.0(12)**	1422.7 (A)	1396.7	1372.2 (A_u)
ν_{27}	NH_2 bend **49.4(28) + 18.7(25) + 9.4(26) + 9.4(19)**	1537.5 (B)	1430.6	1435.5 (A_g)
ν_{28}	$H_{14}-N_4-C_1-N_3-H_{11}$ bend + C−C str. **76.4(10) + 6.8(1) + 5.5(15)**	1587.7 (A)	1645.4	1587.4 (A_g)
ν_{29}	NH_2 bend **48.3(27) + 17.0(28) + 9.5(19) + 7.9(33) + 6.7(25) + 6.3(34)**	1676.9 (B)	1690.4	1603.0 (A_u)
ν_{30}	NH_2 bend +C−C str **72.4(11) + 6.3(1) + 5.2(16)**	1713.6 (A)	1781.0	1708.1(A_g)
ν_{31}	asym. N−O str. +skelet.def **22.9(23) + 21.5(24) + 15.0(30) + 14.5(29) + 9.3(26) + 6.8(28)**	1751.8 (B)	1789.6	1768.5 (A_u)
ν_{32}	sym. NO str.+skelet.def **22.8(6) + 20.3(7) + 19.8(13) + 17.9(12) + 7.7(9)**	1770.1 (A)	1833.6	1776.0 (A_g)
ν_{33}	N_4−H sym str+N_3−H sym **75.1(21) + 23.9(20)**	3599.4 (B)	3573.2	3627.0 (A_u)
ν_{34}	N_4−H sym str+N_3−H sym **75.4(4) + 23.4(3)**	3608.8 (A)	3604.3	3632.2 (A_g)
ν_{35}	N_4−H asym str+N_3−H asym **73.6(3) + 24.6(4)**	3775.6 (A)	3666.5	3773.1 (A_g)
ν_{36}	N_4−H asym str+N_3−H asym **73.3(20) + 25.0(21)**	3776.3 (B)	3740.7	3774.2 (A_u)

[a] The assignment is based on the values determined for FOX-7. The legend of abbreviations used in text is as follows: def = deformation; str = strectching; assym = asymmetric; symm = symmetric. The vibrational modes are further characterized in terms of the potential energy distribution (in percent.) The numbers in parentheses refer to the symmetry coordinates defined below. Symmetry coordinates contributing less than five percent are omitted. Symmetry coordinate definitions (ν, α, and ω denote bond stretches, angle bends, and torsions, respectively) are as follows: $S_1 = \nu(C_1-C_2)$, $S_2 = \nu(C_1-N_3 + C_1-N_4)$, $S_3 = \nu(N_3-H_{11} + N_4-H_{14})$, $S_4 = \nu(N_3-H_{12} + N_4-H_{13})$, $S_5 = \nu(C_2-N_5 + C_2-N_6)$, $S_6 = \nu(N_5-O_7 + N_6-O_9)$, $S_7 = \nu(N_5-O_8 + N_6-O_{10})$, $S_8 = \alpha(N_3-C_1-C_2 + N_4-C_1-C_2)$, $S_9 = \alpha(N_5-C_2-C_1 + N_6-C_2-C_1)$, $S_{10} = \alpha(H_{11}-N_3-C_1 + H_{14}-N_4-C_1)$, $S_{11} = \alpha(H_{12}-N_3-C_1 + H_{13}-N_4-C_1)$, $S_{12} = \alpha(O_7-N_5-C_2 + O_9-N_6-C_2)$, $S_{13} = \alpha(O_8-N_5-C_2 + O_{10}-N_6-C_2)$, $S_{14} = \omega(N_3-C_1-C_2-N_5 + N_4-C_1-C_2-N_6)$, $S_{15} = \omega(H_{11}-N_3-C_1-C_2 + H_{14}-N_4-C_1-C_2)$, $S_{16} = \omega(H_{12}-N_3-C_1-C_2 + H_{13}-N_4-C_1-C_2)$, $S_{17} = \omega(O_7-N_5-C_2-C_1 + O_9-N_6-C_2-C_1)$, $S_{18} = \omega(O_8-N_5-C_2-C_1 + O_{10}-N_6-C_2-C_1)$, $S_{19} = \nu(C_1-N_3 - C_1-N_4)$, $S_{20} = \nu(N_3-H_{11} - N_4-H_{12})$, $S_{21} = \nu(N_3-H_{12} - N_4-H_{13})$, $S_{22} = \nu(C_2-N_5 - C_2-N_6)$, $S_{23} = \nu(N_5-O_7 - N_6-O_9)$, $S_{24} = \nu(N_5-O_8 - N_6-O_{10})$, $S_{25} = \alpha(N_3-C_1-C_2 - N_4-C_1-C_2)$, $S_{26} = \alpha(N_5-C_2-C_1 - N_6-C_2-C_1)$, $S_{27} = \alpha(H_{11}-N_3-C_1 - H_{14}-N_4-C_1)$, $S_{28} = \alpha(H_{12}-N_3-C_1 - H_{13}-N_4-C_1)$, $S_{29} = \alpha(O_7-N_5-C_2 - O_9-N_6-C_2)$, $S_{30} = \alpha(O_8-N_5-C_2 - O_{10}-N_6-C_2)$, $S_{31} = \omega(C_1-C_2-N_5-N_6)$, $S_{32} = \omega(N_3-C_1-C_2-N_5 - N_4-C_1-C_2-N_6)$, $S_{33} = \omega(H_{11}-N_3-C_1-C_2 - H_{14}-N_4-C_1-C_2)$, $S_{34} = \omega(H_{12}-N_3-C_1-C_2 - H_{13}-N_4-C_1-C_2)$, $S_{35} = \omega(O_7-N_5-C_2-C_1 - O_9-N_6-C_2-C_1)$, $S_{36} = \omega(O_8-N_5-C_2-C_1 - O_{10}-N_6-C_2-C_1)$.

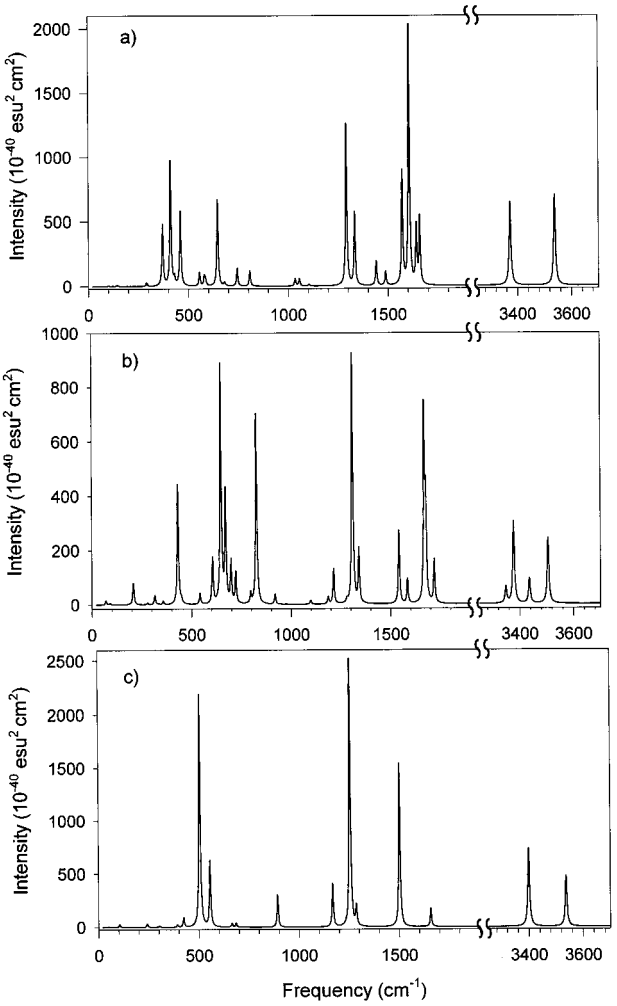

Figure 3. Infrared spectra of (a) the FOX-7, (b) 1,2-*cis*, and (c) 1,2-*trans* FOX-7 molecules calculated at the MP2/6-31G** level.

dinates. Exceptions include the N−H stretching modes (ν_{33}−ν_{36}) and five N−H deformation modes (ν_8, ν_9, ν_{12}, ν_{13}, and ν_{14}), which are dominated by motions along a single symmetry coordinate.

B. Ab Initio Total Energy Calculations. *B1. Geometric and Electronic Properties of FOX-7 Crystal.* We have also investigated the bulk structure of crystalline FOX-7 by carrying out ab initio total energy calculations. The relaxation of the unit cell was done with respect to the independent lattice parameters allowed by $P2_1/n$ space group symmetry, namely, the crystal dimensions *a*, *b*, and *c* and the angle β of the unit cell, whereas the other two angles were kept at 90.0°. The results of these calculations are given in Table 3. We have also included for comparison in Table 3 the experimental X-ray crystal data obtained by Bemm et al.[5] (Exp1) and Gilardi[6] (Exp2).

There exist some small differences in the two sets of experimental lattice parameters, Exp1[5] and Exp2[6] in Table 3, with a maximum deviation of 1.2% for lattice dimension *b*. Our results are closer to the values reported by Gilardi[6] (Exp2) and consequently we discuss our results relative to them. The analysis of the calculated results indicates that the agreement with the experimental values is good. For the cutoff distance of 600 eV the errors relative to the experimental values for cell dimensions are small with values of 0.55%, 2.08% and −0.04% for *a*, *b*, and *c*, respectively. There is similar very good agreement for the lattice angle β, with a difference of only 0.18%. We have also investigated the effects of removal of the $P2_1/n$ symmetry constraints and found that the final optimized structure does not change significantly from the above values.

The calculated geometry of FOX-7 is compared with the experimental data, Exp1[5] and Exp2,[6] in Table 3. The experimental intramolecular geometrical parameters are also well reproduced by the computations with maximum deviations of 2.5% for bond lengths and 2.1% for bond angles. In particular, it is found that the predicted molecular configuration of the C and N atoms is essentially planar, except for the nitro-N atoms, particularly N(5), which are out of the plane. Indeed, as illustrated by the data in Table 3, the magnitude of torsional angles $\tau(C_1-C_2-N_5-O_8)$ and $\tau(C_1-C_2-N_5-O_7)$ indicate much larger out-of-plane rotations for the N_5-nitro group than is the case for the rotations of the N_6-nitro group, as described by the angles $\tau(C_1-C_2-N_6-O_9)$ and $\tau(C_1-C_2-N_6-O_{10})$. This asymmetry of the two nitro groups is in contrast with the results obtained for the isolated molecule where the two groups are equivalent and have equal out-of-plane rotations. Additionally, relative to the calculated gas-phase structure the C═C bond is elongated in the crystalline phase by about 0.04 Å, because of the strong intermolecular interactions.

When the predicted and experimental bond distances in Table 3 are compared, it can be seen that the largest deviations appear for the N−H bonds as well as for the N−H···O hydrogen bonds. For N−H bonds our calculations indicate values around 1.01−1.02 Å, whereas the experimental values vary from 0.83 to 0.88 Å. Similarly, the predicted N−H···O interatomic distances range between 1.88 and 2.46 Å, which are smaller than the experimental values that vary from 2.18 to 2.54 Å. The main reason for such differences is the uncertainty in the H-atom positions obtained using X-ray diffraction, which determines the centers of charge for H atoms and not the positions of the nuclei. Additionally, we observe in agreement with the experiment that every H atom in the amino group is involved in two hydrogen bonds: one shorter (stronger) than the other. The shortest hydrogen bonds, indicated with an asterisk in Table 3, are intramolecular, whereas the other bonds are intermolecular. This extensive intramolecular and intermolecular hydrogen bonding network was found to be responsible for the limited amount of thermal motion of the individual atoms as well as for the low sensitivity to friction and impact of the FOX-7 crystal.[5]

We have calculated the self-consistent band structure for the optimized structure of the FOX-7 crystal. The result is shown in Figure 4, and the corresponding total densities of states are given in Figure 5. In Figures 4 and 5, the energy of the highest occupied crystalline orbital has been set to zero. As can be seen, FOX-7 is an electrical insulator with a band gap at the Γ point of 2.2 eV.

A better understanding of the character of these bands can be obtained by projecting the calculated charge density on the atom-centered orbitals. These representations, called the projected density of states (PDOS), are given in Figure 5 for individual atoms C_1, C_2, N_3, N_5, O_7, O_8, H_{11}, and H_{12} in the FOX-7 molecule. The individual s and p bands corresponding to the various atoms can be identified clearly in the total DOS spectrum except in the regions between (−8, −6) eV and (−2, −1) eV where there is a mixing of states, consistent with the molecular character of the crystal. A comparison of the results in Figure 5a−e shows that the top of the valence band is represented by the O(2p), N_3(2p), and C_2(2p) levels. The bottom of the conduction band or the lowest unoccupied crystalline orbitals between 1.5 and 2 eV are formed by contributions from both O(2p) and N_5(2p) of the nitro groups.

TABLE 3: Comparison of the Crystallographic and Molecular Geometrical Parameters for FOX-7 in the Crystal Phase as Obtained from Plane-Wave ab Initio Calculations with the Corresponding Experimental Data

cutoff energy (eV)	*a* (Å)	*b* (Å)	*c* (Å)	α (degrees)	*β* (degrees)	*γ* (degrees)	volume (Å^3)
495.0	6.9863 (0.67)[c]	6.8334 (2.95)	11.3654 (0.21)	90.0	90.915 (0.33)	90.0	542.522 (3.86)
600.0	6.9783 (0.55)	6.7758 (2.08)	11.3358 (−0.04)	90.0	90.796 (0.18)	90.0	535.952 (2.60)
Exp1[a]	6.9410	6.5600	11.3150	90.0	90.555	90.0	515.888
Exp2[b]	6.9397	6.6374	11.3406	90.0	90.611	90.0	522.328

	calcd	Exp1	Exp2		calcd	Exp1	Exp2
	Bond Distances (Å)				Bond Angles (degree)		
$r(C_1-C_2)$	1.4649 (1.3)[c]	1.4558 (0.7)	1.4460	$\theta(N_3-C_1-N_4)$	118.22 (0.1)	118.42 (0.1)	118.27
$r(C_1-N_3)$	1.3364 (1.0)	1.3254 (0.2)	1.3233	$\theta(N_3-C_1-C_2)$	120.70 (0.2)	120.72 (0.2)	120.42
$r(C_1-N_4)$	1.3308 (1.6)	1.3191 (0.7)	1.3097	$\theta(N_4-C_1-C_2)$	121.04 (0.5)	120.82 (0.4)	121.25
$r(C_2-N_5)$	1.4231 (0.3)	1.4269 (0.6)	1.4188	$\theta(N_5-C_2-N_6)$	116.68 (0.6)	116.32 (0.3)	115.94
$r(C_2-N_6)$	1.4098 (0.7)	1.3983 (0.1)	1.3997	$\theta(N_5-C_2-C_1)$	119.85 (0.3)	119.74 (0.4)	120.27
$r(N_5-O_7)$	1.2622 (2.5)	1.2424 (0.9)	1.2314	$\theta(N_6-C_2-C_1)$	123.46 (0.2)	123.89 (0.1)	123.75
$r(N_5-O_8)$	1.2707 (1.9)	1.2489 (0.2)	1.2467	$\theta(O_7-N_5-O_8)$	120.62 (0.0)	121.04 (0.3)	120.65
$r(N_6-O_9)$	1.2621 (2.5)	1.2424 (0.9)	1.2314	$\theta(O_7-N_5-C_2)$	120.55 (0.4)	120.33 (0.5)	120.99
$r(N_6-O_{10})$	1.2640 (2.3)	1.2416 (0.4)	1.2364	$\theta(O_8-N_5-C_2)$	118.81 (0.4)	118.60 (0.2)	118.32
$r(N_3-H_{11})$	1.0239 (19.5)	0.8821 (3.0)	0.8565	$\theta(O_9-N_6-O_{10})$	120.69 (0.3)	120.87 (0.1)	120.96
$r(N_3-H_{12})$	1.0186 (18.0)	0.8710 (0.9)	0.8631	$\theta(O_9-N_6-C_2)$	120.72 (0.2)	120.13 (0.2)	120.39
$r(N_4-H_{13})$	1.0185 (11.6)	0.8403 (7.9)	0.9125	$\theta(O_{10}-N_6-C_2)$	119.02 (0.1)	118.92 (0.3)	118.58
$r(N_4-H_{14})$	1.0221 (24.1)	0.8379 (1.7)	0.8235	$\theta(H_{11}-N_3-H_{12})$	118.28 (2.1)	118.18 (2.0)	115.87
				$\theta(H_{11}-N_3-C_1)$	119.68 (1.6)	119.63 (1.6)	121.63
				$\theta(H_{12}-N_3-C_1)$	121.50 (0.6)	121.67 (0.5)	122.27
				$\theta(H_{13}-N_4-H_{14})$	119.33 (0.2)	118.15 (1.2)	119.54
				$\theta(H_{13}-N_4-C_1)$	120.36 (0.1)	120.97 (0.4)	120.43
				$\theta(H_{14}-N_4-C_1)$	120.24 (0.2)	120.89 (0.7)	120.00
	Dihedral Angles (degree)				Hydrogen-Bonding Distances (Å)[d]		
$\tau(N_4-C_1-C_2-N_5)$	177.82	172.91	172.82	N4−H14...O9	2.02	2.18	2.19
$\tau(N_3-C_1-C_2-N_6)$	173.85	177.79	177.57	N4−H14...O8	2.46	2.50	2.54
$\tau(N_4-C_1-C_2-N_5)$	−4.86	−4.68	−4.76	N4−H13...O10*	1.88	1.97	1.96
$\tau(C_1-C_2-N_6-O_9)$	−169.86	−171.00	−170.80	N4−H13...O7	2.20	2.29	2.32
$\tau(C_1-C_2-N_6-O_{10})$	6.78	5.80	6.34	N3−H11...O7	2.00	2.17	2.18
$\tau(C_1-C_2-N_5-O_7)$	−145.89	−143.57	−144.33	N3−H11...O9	2.29	2.46	2.49
$\tau(C_1-C_2-N_5-O_8)$	32.41	34.29	33.95	N3−H12...O8*	1.92	2.03	1.98
$\tau(N_5-C_2-N_6-O_9)$	11.40	11.40	11.44	N3−H12...O10	2.25	2.36	2.32
$\tau(N_5-C_2-N_6-O_{10})$	−148.80	−148.00	−148.20				
$\tau(N_6-C_2-N_5-O_7)$	32.90	34.14	33.52				
$\tau(N_6-C_2-N_6-O_8)$	−148.80	−148.00	−148.20				
$\tau(C_2-C_1-N_4-H_{13})$	−2.23	−0.56	−1.23				
$\tau(C_2-C_1-N_4-H_{14})$	179.21	179.50	−179.84				
$\tau(C_2-C_1-N_3-H_{11})$	−179.12	178.34	177.78				
$\tau(C_2-C_1-N_3-H_{12})$	−9.41	−10.08	−7.83				
$\tau(H_{11}-N_3-C_1-N_4)$	−1.72	0.69	0.12				
$\tau(H_{14}-N_4-C_1-N_3)$	−1.82	−2.85	−2.21				
$\tau(H_{12}-N_3-C_1-N_4)$	173.19	172.27	174.51				
$\tau(H_{13}-N_4-C_1-N_3)$	174.51	177.08	176.41				

[a] Exp1, data from ref 5. [b] Exp2, data from ref 6. [c] The values in parentheses correspond to percentage differences relative to Exp2 values. [d] The intramolecular hydrogen bonds are indicated with an asterisk.

C. Molecular Packing Calculations. The intermolecular potential parameters used to describe the physical properties of the FOX-7 crystal together with the corresponding set of electrostatic charges assigned to the atoms are presented in Table 4. The results of the molecular packing calculations obtained using the potential parameters given in Table 1 are summarized in Table 5.

For all of the cases in Table 4, the symmetry space group was maintained as we verified by the existent symmetry relations of the $P2_1/n$ space group between the $Z - 1$ molecules in the unit cell and the corresponding central molecule with $Z = 1$.

The changes in lattice parameters and molecular orientations after energy minimization relative to the experimental structures[5,6] are also given in parentheses in Table 5 where they are denoted as LMIN1 and LMIN2, respectively. Relative to the structure found by Bemm[5] the maximum deviations of the lattice dimensions is 1.83%. Similarly, by considering as reference the parameters found by Gilardi,[6] our predictions indicate variations of less than 1.61%. Also, in both cases, the predicted unit cell angles are very close to the experimental values, with maximum deviation for the β angle being 0.43% and 0.47% relative to the Bemm[5] and Gilardi[6] results. There is essentially no change in the values of the angles α and γ, which remain close to 90°, consistent with the space group symmetry. Moreover, there are only small translations of the molecules in the asymmetric unit cell, whereas the variations of the Euler angles that describe the molecular orientation in the unit cell have changes of less than 3.5%.

We also list in Table 5 the total lattice energies for the minimized configurations decomposed into nonbonded and electrostatic contributions. The contributions of these two types of energies to the total lattice energy are in the ratio of 0.42: 0.58. For the minimized lattices, the total energies are $U = -115.707$ kJ/mol for the LMIN1 model and $U = -114.739$ kJ/mol for the LMIN2 model. In both cases, the predicted lattice energies are in good agreement with the value of −113.81 kJ/mol, determined from the heat of sublimation found by Politzer et al.[9]

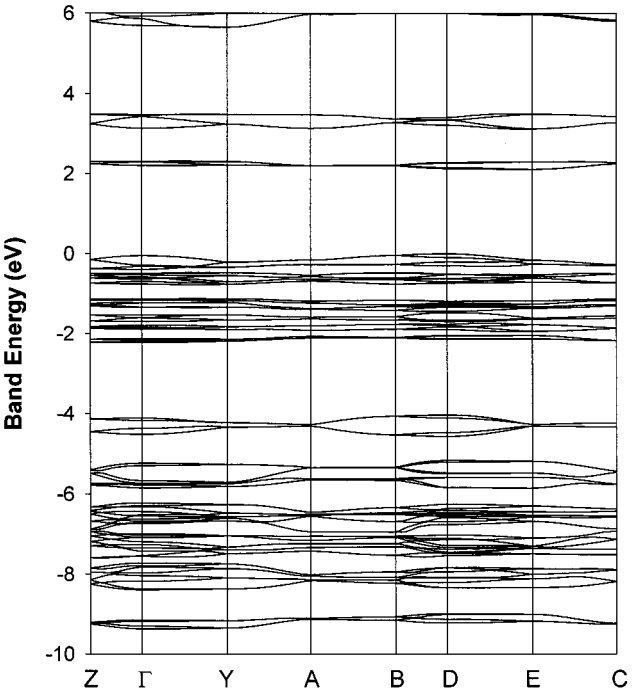

Figure 4. Calculated band structure of the FOX-7 structure along different symmetry directions of the Brillouin zone.

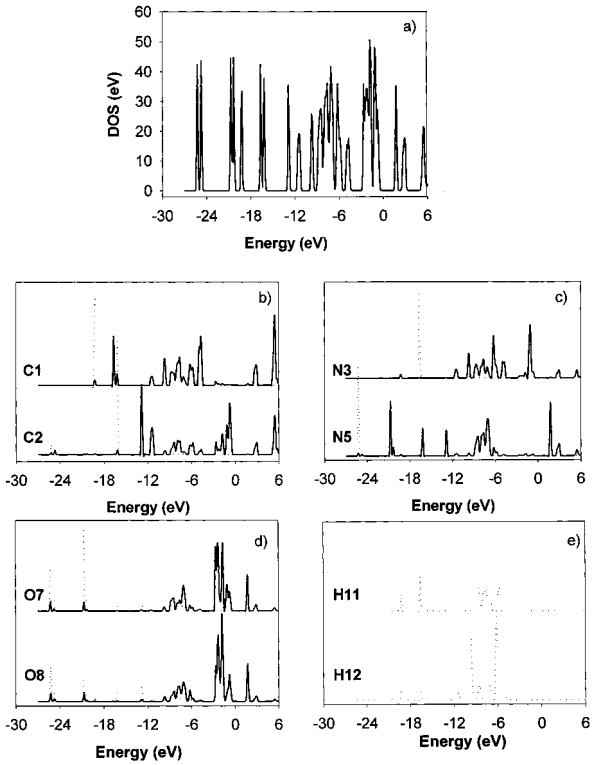

Figure 5. Calculated density of states for the FOX7 crystal (panel a) together with the projected density of states for the C_1, C_2, N_3, N_5, O_7, O_8, H_{11}, and H_{12} atoms indicated in panels b−e. The dotted and continuous lines in panels b−e represent the s and p bands, respectively.

These results suggest that the proposed model potential is an effective pair potential able to reproduce both the crystallographic parameters of a FOX-7 crystal as well as its lattice energy. For this reason, such a potential can be used to provide an accurate description of the equilibrium properties of a FOX-7 crystal at least in the region of low temperatures. Given the fitting procedure we used to develop this potential, many-body contributions to the interactions are indirectly represented in the present analytic form.

TABLE 4: Force Field Parameters for Crystalline FOX-7

atom[a]	charge (|e|)
C_1	0.838 068
C_2	−0.542 662
N_3	−0.952 801
N_4	−0.926 461
N_5	0.754 325
N_6	0.710 244
O_7	−0.358 760
O_8	−0.471 171
O_9	−0.355 147
O_{10}	−0.490 010
H_{11}	0.434 253
H_{12}	0.464 860
H_{13}	0.476 296
H_{14}	0.418 966

pair ($\alpha-\beta$)	$A_{\alpha\beta}$ (kJ/mol)[a]	$B_{\alpha\beta}$ ($Å^{-1}$)	$C_{\alpha\beta}$ (kJ/(mol $Å^6$))
H−H	9213.51	3.74	136.3800
C−C	369 726.33	3.60	2439.3459
N−N	568 859.00	3.78	1378.4000
O−O	273 92.00	3.59	836.0300

[a] For mixed interactions the following combination rules have been used: $A_{\alpha\beta} = \sqrt{A_{\alpha\alpha}A_{\beta\beta}}$, $B_{\alpha\beta} = (B_{\alpha\alpha} + B_{\beta\beta})/2$, and $C_{\alpha\beta} = \sqrt{C_{\alpha\alpha}C_{\beta\beta}}$.

D. NPT Molecular Dynamics Calculations. A more realistic prediction of the structural lattice parameters can be obtained by considering the molecular motion as a function of temperature and pressure. For this purpose, we have determined the structural crystal parameters at atmospheric pressure and in the temperature range of 4.2−450 K. These results are summarized in Table 6.

As can be seen by comparing the data in Tables 5 and 6, the lattice dimensions obtained at $T = 4.2$ K are in very close agreement with those determined in the molecular packing calculations without symmetry constraints. This is expected because the thermal effects at 4.2 K should be minimal and the thermal averages at this temperature should be close to the values corresponding to the potential energy minimum. At 273 K, the average lattice dimensions of these crystals agree satisfactorily with the experimental values measured at 273 K,[5,6] the corresponding differences for the *a*, *b*, and *c* lattice dimensions being 1.0% (1.4%), 2.7% (2.8%), and 0.7% (0.8%), respectively. Moreover, in both low and ambient temperature simulations, the unit cell angles α and γ remain approximately equal to 90°, whereas the β angle vary slightly from 90.118° at 4.2 K to 89.576° over the temperature range of 4.2−450 K.

In Figure 6, we indicate the temperature dependence of the COM RDFs. It is evident from these results that increasing the temperature from 4.2 to 400 K does not produce any significant displacements of the molecular COM. Indeed, the RDFs at these temperatures correspond to well ordered structures with correlation at long distances. The positions of the major peaks do not change significantly, and the main temperature effect is the broadening of the peaks with partial overlapping of some of them.

Further insight into the crystallographic structure can be obtained by analyzing the site−site RDFs for the intermolecular hydrogen bonds $N_3-H_{11}\cdots O_7$ and $N_3-H_{12}\cdots O_{10}$. These RDFs were calculated as averages over all molecules in the MD box but limited by the cutoff distance used in the potential

TABLE 5: Lattice Parameters and Energies from Crystal Packing Calculations without Symmetry Constraints (LMIN1 and LMIN2) Obtained Using the Molecular Structures Determined in Ref 5 (EXP1) and Ref 6 (EXP2), Respectively[a]

	lattice energy[b]		lattice parameters[c]					
	NB	ES	*a*	*b*	*c*	α	*β*	*γ*
EXP1	−113.81[d]		6.93967	6.6374	11.3406	90.000	90.611	90.000
EXP2	−113.81		6.941	6.569	11.315	90.000	90.550	90.000
LMIN1	−47.992	−67.715	6.8527	6.6523	11.5219	90.018	90.120	90.023
			(−1.27)	(1.27)	(1.83)	(0.02)	(−0.47)	(0.03)
LMIN2	−48.075	−66.664	6.8281	6.6494	11.5080	90.021	90.224	90.012
			(−1.61)	(0.18)	(1.48)	(0.02)	(−0.43)	(0.01)

	Δ*x*[e]	Δ*y*	Δ*z*	ΔΦ (degree)[f]	ΔΨ (degree)	ΔΘ (degree)
LMIN1	−0.197	0.017	−0.002	2.115	1.935	3.187
LMIN2	−0.185	0.026	−0.004	2.590	1.778	3.552

[a] The percentage change in lattice and molecular parameters after energy minimization is determined as a function of the respective experimental geometries and is given in parentheses. [b] Nonbonded (NB) and electrostatic (ES) lattice energies per molecule in kJ/mol. [c] Lattice dimensions *a*, *b*, and *c* in angstroms and angles α, *β*, and *γ* in degrees. [d] Lattice energy estimated using the theoretical heat of sublimation of −108.784 kJ/mol as provided by P. Politzer (ref 9). [e] Change in fractional coordinates of molecular centroids. [f] Change in Euler angles of molecular centroids.

TABLE 6: Lattice Parameters Obtained in NPT-MD Calculations for FOX-7 as a Function of Temperature[a]

	lattice dimensions						
T (K)	*a* (Å)	*b* (Å)	*c* (Å)	α (degrees)	*β* (degrees)	*γ* (degrees)	volume (Å^3)
4.2	6.8532	6.65451	11.5241	90.000	90.118	90.000	525.5625
25.0	6.8571	6.66345	11.5382	90.001	90.107	90.013	527.1875
50.0	6.8614	6.67857	11.5481	89.999	90.089	90.013	529.1875
75.0	6.8679	6.69561	11.5510	90.020	90.065	90.048	531.1666
100.0	6.8754	6.71135	11.5543	90.003	90.026	90.042	533.1458
125.0	6.8822	6.72965	11.5564	89.989	90.001	90.037	535.2291
150.0	6.8903	6.74492	11.5639	89.995	89.965	90.047	537.4375
175.0	6.8952	6.76514	11.5727	90.003	89.954	89.985	539.8333
200.0	6.9030	6.78033	11.5802	89.966	89.910	90.018	542.0000
220.0	6.9071	6.79629	11.5881	90.080	89.993	89.986	543.9791
250.0	6.9164	6.82263	11.5911	90.020	89.856	89.942	546.9583
273.0	6.9242	6.83572	11.6054	90.037	89.919	90.091	549.2916
300.0	6.9304	6.86496	11.6082	89.996	89.790	89.981	552.2708
325.0	6.9384	6.88374	11.6215	90.023	89.726	90.010	555.0625
350.0	6.9505	6.90081	11.6303	90.027	89.737	90.044	557.8125
375.0	6.9570	6.92543	11.6463	89.906	89.676	90.037	561.1041
400.0	6.9660	6.95408	11.6481	89.965	89.644	89.970	564.2500
425.0	6.9806	7.01608	11.6669	90.044	89.576	90.067	571.3750
450.0	6.9947	7.04177	11.6762	89.962	89.576	90.042	575.0833
χ	45.7×10^{-6}	129.6×10^{-6}	29.2×10^{-6}				204.8×10^{-6}

[a] The calculated thermal expansion coefficients (*χ*) at 273 K are also indicated. The units for the linear and volume expansion coefficients are K^{-1}.

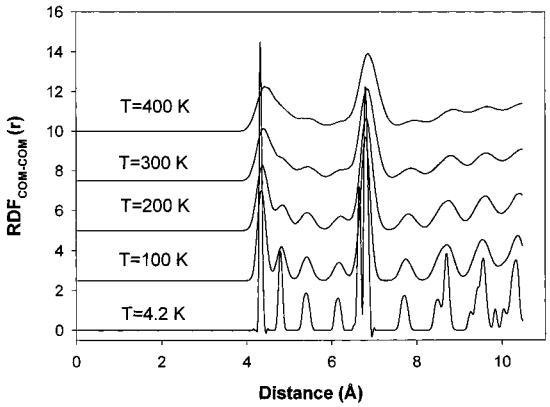

Figure 6. Radial distribution functions (RDF) for molecular center-of-mass to center-of-mass (COM−COM) sites as functions of temperature at atmospheric pressure.

calculation. The results are shown in Figure 7. It can be seen that increasing the temperature does not dramatically alter the individuality of the main peaks, indicating the lack of rotational disorder.

In Figure 8, we present the variation of the lattice dimensions and unit cell volume with temperature. The corresponding linear and volume expansion coefficients determined from these dependencies at 273 K are indicated in Table 6. It can be seen that there is an anisotropic thermal expansion of the crystal, with the largest occurring along the *b* axis. This behavior can be understood by analyzing the crystallographic structure of FOX-7, as illustrated in Figure 1b. Indeed, the molecular packing for FOX-7 crystals presents extensive hydrogen bonding within the wave-shaped layers positioned in the aOc planes, whereas the interactions between planes are of the weaker van der Waalstype. Consequently it is expected that thermal expansion effects are more significant along a direction perpendicular on the hydrogen bonding planes, i.e., along the *b* axis, whereas the expansions along the other two axes are smaller and have similar values.

IV. Concluding Remarks

Ab initio molecular orbital calculations were performed to predict the structures, the fundamental vibrational frequencies, and the relative stabilities of three FOX-7 isomers.

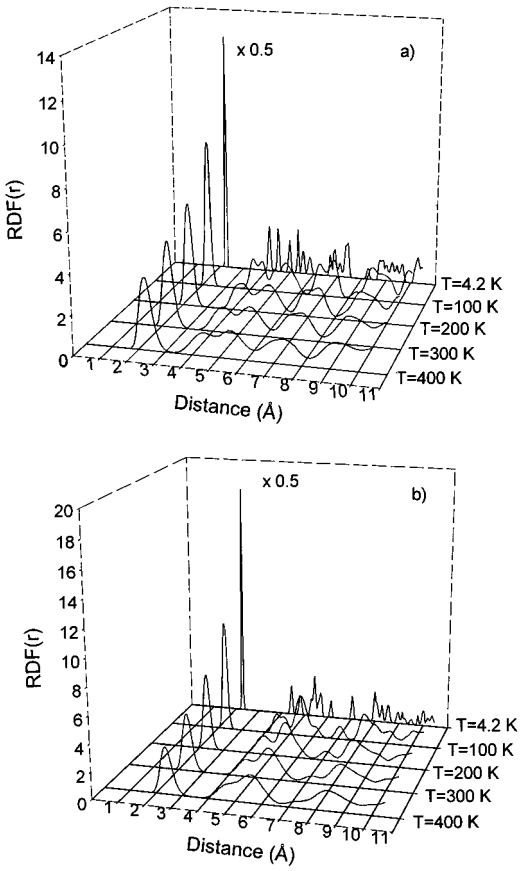

Figure 7. Radial distribution functions (RDF) for (a) $N_3-H_{11}\cdots O_7$ and (b) $N_3-H_{12}\cdots O_{10}$ sites as functions of temperature at atmospheric pressure.

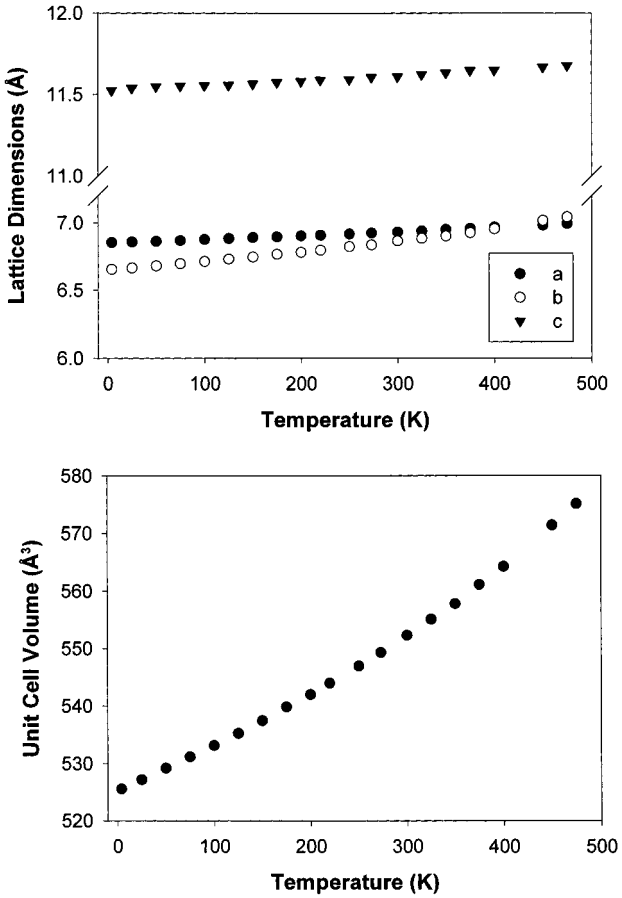

Figure 8. Temperature variation of the lattice dimensions (a) and unit cell volume (b) as function s of temperature from NPT-MD simulations using the rigid-body approximation.

It was found that FOX-7 is the most stable of the three isomers, followed by the 1,2-trans and 1,2-cis isomers. Electronic delocalization and intramolecular hydrogen bonding have been identified as stabilizing factors, the first one being the most important in determining the order of stability of the isomers. Analysis of the geometrical parameters for the FOX-7 molecule indicate that there is relatively good agreement with solid-phase results, except for the twist angles of the NO_2 and NH_2 groups, which are much larger in the gas phase than in the crystalline phase.

We have also shown that reliable geometrical parameters for the FOX-7 crystal can be obtained by using plane-wave total energy calculations based on DFT theory and the pseudopotential method. In particular, in good agreement with experimental findings,[5,6] the calculations predict that in the solid phase the molecular configuration of the C and amino N atoms is essentially planar, whereas the nitro-N atoms, particularly N_5, are out of plane. The calculations provide a better characterization of both the intramolecular and intermolecular hydrogen bonding parameters than that based on X-ray data.[5,6]

We have also investigated the band structure along different Brillouin directions for the FOX-7 crystal and have determined a value of 2.2 eV for the band gap at the Γ point. This value is expected to represent a lower limit of the real band gap of the crystal.

We have developed an intermolecular potential for the FOX-7 crystal on the basis of exp-6 Buckingham potentials and Coulombic interactions. Electrostatic charges were determined from fits to ab initio electrostatic potentials calculated at the MP2/6-31G** level. The values of the N and O intermolecular potential parameters were optimized to minimize the difference between the theoretical and experimental[5,6] structures and their corresponding energies.[9]

A prime test of the proposed potential was done in symmetry unconstrained molecular packing calculations. It was shown that the space group symmetry is maintained throughout energy minimization and that the crystallographic parameters are reproduced within 1.48%. Also, there is a very good agreement between the predicted lattice energy (−114.73 kJ/mol) and previous theoretical evaluations (−113.81 kJ/mol).[9]

The temperature dependencies of the physical parameters of the FOX-7 crystal have been investigated by performing isothermal−isobaric molecular dynamics simulations at zero pressure over the temperature range of 4.2−450 K. The calculated results show that at 273 K the proposed potential model reproduces the experimental unit cell dimensions within 2.8%. Additionally, we found that there is little translational and rotational disorder of the molecules during thermal trajectories.

The linear and volume thermal expansion coefficients of the crystal were determined from the averages of lattice dimensions extracted from trajectory calculations. The results obtained indicate that the largest expansion of the crystal takes place along the *b* axis, corresponding to a direction perpendicular on molecular planes.

This study provides a more comprehensive understanding of the structural, spectroscopic, and energetic characteristics of the FOX-7 molecule in its gaseous and crystalline phases. Furthermore, this work provides the basis for studies of pressure effects on the lattice dynamics and atomic-level modeling of reactions in condensed phases. A further development that is needed is

the development of a general intramolecular and intermolecular potential that describes the crystalline phase of FOX-7 that will allow the analysis of more subtle effects such as those due to pressure compression or reactions in the condensed phases.

Acknowledgment. This work was supported in part by the Air Force Office of Scientific Research (Grant No. F49620-00-l-0273). We gratefully acknowledge the computational resources provided by the ASC MSRC supercomputer center. We would like to thank Dr. Richard D. Gilardi of the Naval Research Laboratory, Washington, DC for making available to us his unpublished crystallographic parameters for the FOX-7 crystal.

Supporting Information Available: Comparison, in Tables 1S−3S, of the geometrical parameters of FOX-7 and its 1,2-cis and 1,2-trans isomers at different molecular orbital calculations. This material is available free of charge via the Internet at http://pubs.acs.org.

References and Notes

(1) Lee, K.-Y.; Storm, C. B.; Hiskey, M. A.; Coburn, M. D. *J. Energ. Mater*. **1991**, *9*, 415.
(2) Lee, K.-Y.; Chapman, L. B.; Coburn, M. D. *J. Energ. Mater*. **1987**, *5*, 27.
(3) Katrizky, A. R.; Cundy, D. J.; Chen, J. *J. Energ. Mater*. **1993**, *11*, 345.
(4) Latypov, N. V.; Bergman, J.; Langlet, A.; Wellmar, U.; Bemm U. *Tetrahedron* **1998**, *54*, 11525.
(5) Bemm, U.; Östmark, H. *Acta Crystallogr*. **1999**, *C54*, 1997.
(6) Gilardi, R. Private communication to the Cambridge Crystallographic Data Center, 1999. Deposition number CCDC 127539.
(7) Cady, H. H.; Larson, A. C. *Acta Cryst*. **1965**, *18*, 485.
(8) Lee, K. -Y.; Gilardi, R. In *Structure and Properties of Energetic Materials*; Lienbenberg, D. H., Armstrong, R. W., GIlman, J. J., Eds.; Materials Research Society: Pittsburgh, PA, 1993; Vol. 296, p 237.
(9) Politzer, P.; Concha, M. C.; Grice, M. E.; Murray, J. S.; Lane, P.; Habibollazadeh, D. *J. Mol. Struct.* (*THEOCHEM*) **1998**, *452*, 75.
(10) Gindulytè, A.; Massa, L.; Huang, L.; Karle, J. *J. Phys. Chem. A* **1999**, *103*, 11045.
(11) Östmark, H.; Langlet, A.; Bergman, H.; Wingborg, N.; Wellmar, U.; Bemm, U. FOX-7- A New Explosive With Low Sensitivity and High Performance; *11th International Symposium on Detonation*, 1998; http://www.sainc.com/onr/detsymp/ financcmt.html.
(12) Möller, C. M. S. *Phys. Rev.* **1934**, *46*, 618. (b) Hehre, W. J.; Ditchfield, R.; Pople, J. A. *J. Chem. Phys.* **1972**, *56*, 2257. (c) Hariharan, P. C.; Pople, J. A. *Theor. Chim. Acta* **1973**, *28*, 213. (d) Gordon, M. S. *Chem. Phys. Lett.* **1980**, *76*, 163.
(13) (a) Hohenber, P.; Kohn, W. *Phys. Rev. B*: *Condens. Matter* **1964**, *126*, 864. (b) Parr, R. G.; Yang, W. *Density-Functional Theory of Atoms and Molecules*; Oxford University Press: New York, 1989.
(14) Sorescu, D. C.; Sutton, T. R. L.; Thompson, D. L.; Beardall, D.; Wight, C. A. *J. Mol. Struct.* **1996**, *384*, 87.
(15) Sorescu, D. C.; Bennett, C. M.; Thompson, D. L. *J. Phys. Chem. A* **1998**, *102*, 10348.
(16) Becke, A. D. *J. Chem. Phys*. **1993**, *98*, 5648.
(17) Lee, C.; Yang, W.; Parr, R. G. *Phys. Rev. B*: *Condens. Matter* **1988**, *41*, 785.
(18) (a) Sorescu, D. C.; Rice, B. M.; Thompson, D. L. *J. Phys. Chem. B* **1997**, *101*, 798. (b) Sorescu, D. C.; Rice, B. M.; Thompson, D. L. *J. Phys. Chem. B* **1998**, *102*, 948. (c) Sorescu, D. C.; Rice, B. M.; Thompson, D. L. *J. Phys. Chem. B* **1998**, *102*, 6692. (d) Sorescu, D. C.; Rice, B. M.; Thompson, D. L. *J. Phys. Chem. A* **1998**, *102*, 8386. (e) Sorescu, D. C.; Rice, B. M.; Thompson, D. L. *J. Phys. Chem. A* **1999**, *103*, 989.
(19) Frisch, M. J.; Trucks, G. W.; Schlegel, H. B.; Scuseria, G. E.; Robb, M. A.; Cheeseman, J. R.; Zakrzewski, V. G.; Montgomery, J. A., Jr.; Stratmann, R. E.; Burant, J. C.; Dapprich, S.; Millam, J. M.; Daniels, A. D.; Kudin, K. N.; Strain, M. C.; Farkas, O.; Tomasi, J.; Barone, V.; Cossi, M.; Cammi, R.; Mennucci, B.; Pomelli, C.; Adamo, C.; Clifford, S.; Ochterski, J.; Petersson, G. A.; Ayala, P. Y.; Cui, Q.; Morokuma, K.; Malick, D. K.; Rabuck, A. D.; Raghavachari, K.; Foresman, J. B.; Cioslowski, J.; Ortiz, J. V.; Stefanov, B. B.; Liu, G.; Liashenko, A.; Piskorz, P.; Komaromi, I.; Gomperts, R.; Martin, R. L.; Fox, D. J.; Keith, T.; Al-Laham, M. A.; Peng, C. Y.; Nanayakkara, A.; Gonzalez, C.; Challacombe, M.; Gill, P. M. W.; Johnson, B. G.; Chen, W.; Wong, M. W.; Andres, J. L.; Head-Gordon, M.; Replogle, E. S.; Pople, J. A. *Gaussian 98*, revision A.7; Gaussian, Inc.: Pittsburgh, PA, 1998.
(20) Hehre, W.; Radom, L.; Schleyer, P. v. R.; Pople, J. A. *Ab Initio Molecular Orbital Theory*; Wiley-Interscience: New York, 1986.
(21) (a) Scott, A. P.; Radom, L. *J. Phys. Chem*. **1996**, *100*, 16502. (b) Foresman, J. B.; Frisch, A. *Exploring Chemistry with Electronic Structure Methods*; Gaussian, Inc.: Pittsburgh, PA, 1996. (c) Riggs, N. V.; Zoller, U.; Nguyen, M. T.; Radom, L. *J. Am. Chem. Soc*. **1992**, *114*, 4354.
(22) Pulay, P.; Török, F. *Acta Chim. Acad. Sci. Hung*. **1966**, *47*, 273.
(23) Milman, V.; Lee, M. H. *J. Phys. Chem*. **1996**, *100*, 6093.
(24) (a) Chall, M.; Winkler, B.; Milman, V. *J. Phys. Condens. Matter* **1996**, *8*, 9049. (b) Allan, D. R.; Clark, S. J.; Brugmans, M. J. P.; Ackland, G. J.; Vos, W. L. *Phys. Rev. B* **1998**, *58*, 11809.
(25) Sorescu, D. C.; Thompson, D. L. *J. Phys. Chem. B* **1999**, *103*, 6774.
(26) Perdew, J. P. *Phys. Rev. B* **1986**, *33*, 8822; **1986**, *34*, 7406 (E).
(27) Perdew, J. P.; Wang, Y. *Phys. Rev. B* **1986**, *33*, 8800.
(28) Vanderbilt, D. *Phys. Rev. B* **1990**, *41*, 7892.
(29) Kresse, G.; Hafner, J. *J. Phys. Cond. Matter* **1994**, *6*, 8245.
(30) Monkhorst, H. J.; Pack, J. D. *Phys. Rev. B* **1976**, *13*, 5188.
(31) Kresse, G.; Hafner, J. *Phys. Rev. B* **1993**, *48*, 13115.
(32) Kresse, G.; Hafner, J. *Comput. Mater. Sci*. **1996**, *6*, 15.
(33) Kresse, G.; Hafner, J. *Phys. Rev. B* **1996**, *54*, 11169.
(34) Pertsin, A. J.; Kitaigorodsky, A. I. *The Atom−Atom Potential Method, Applications to Organic Molecular Solids*; Springer-Verlag: Berlin, Germany, 1987.
(35) Gibson, K. D.; Scheraga, H. A. *J. Phys. Chem*. **1995**, *99*, 3752.
(36) Gibson, K. D.; Scheraga, H. A. *LMIN*: A Program for Crystal Packing, QCPE, No. 664.
(37) *International Tables for Crystallography*; Hahn, T., Ed.; Reidel: Dordrecht, The Netherlands, 1983.
(38) *Fundamentals of Crystallography*; Giacovazzo, C., Ed.; Oxford University Press: New York, 1992.
(39) Melchionna, S.; Ciccotti, G.; Holian, B. L. *Mol. Phys.* **1993**, *78*, 533.
(40) DL_POLY is a package of molecular simulation routines written by W. Smith and T. R. Forester, copyright The Council for the Central Laboratory of the Research Councils, Daresbury Laboratory at Daresbury, Nr. Warrington, 1996.
(41) Allen, M. P.; Tindesley, D. J. *Computer Simulation of Liquids*; Oxford University Press: New York, 1989.
(42) Fincham, D. *Mol. Simul.* **1992**, *8*, 165.